

Supplementary information for:

Intermediate Wetting State at Nano/Microstructured Surfaces

Gyoko Nagayama*, Dejian Zhang

Department of Mechanical Engineering, Kyushu Institute of Technology, Sensui 1-1,
Tobata, Kitakyushu, Fukuoka 804-8550, Japan

*Corresponding Author:

Gyoko Nagayama

Email: nagayama.gyoko725@mail.kyutech.jp

1. Schematic view of the anodic etching apparatus

The schematic view of the anodic etching apparatus is shown in Fig. s1. The detailed anodic etching condition can be found in Refs. 11 and 12. The anodization power is supplied by a direct current power (AD-8735, AND, Japan). Ammeter with a resolution of 0.0001 mA is used to monitor current (CDM-6000, CUSTOM, Japan). A metal halide light source generator (MME-250, MORETEX, Japan) is installed using a straight light guide (MSG6-1100S-RM, MORITEX, Japan) attached to a condenser lens (ML-70, MORITEX, Japan).

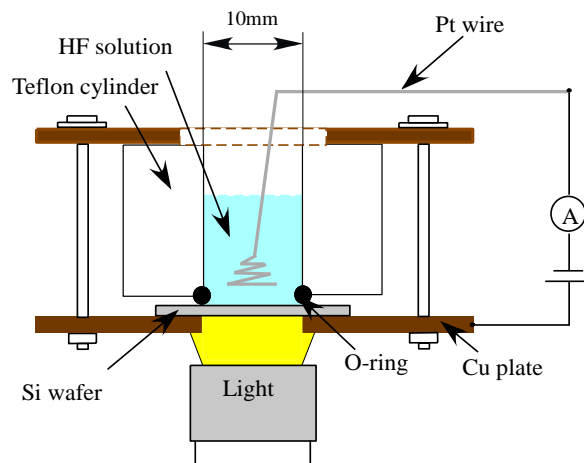


Fig. s1 Experimental apparatus of anodic etching.

2. Solid fraction at structured Si surfaces

We prepared 83 samples (42 porous Si surfaces, 29 patterned Si surfaces and 12 hierarchical nano/microstructured surfaces) for experimental measurement. The solid fraction at the structured surface is determined as follows:

$$\Phi = 1 - \frac{A_{\text{pore}}}{A} \quad (\text{a})$$

where A_{pore} is the summation of the pore area in a given area A . The solid fraction at the patterned surface is determined by the structure parameters of a and s simply, while that at the porous surface is obtained separately using the image analysis. For the hierarchical structured surface, the solid fraction is determined same to the patterned surface.

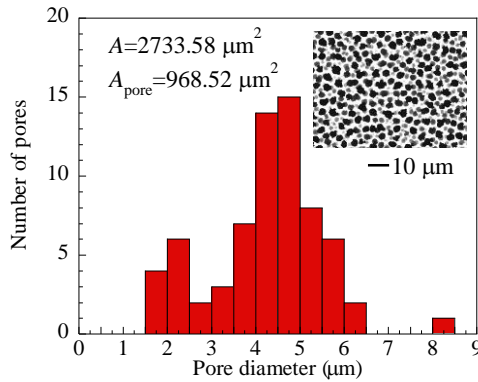


Fig. s2 Surface image of porous Si and its histogram of pore diameter distribution.

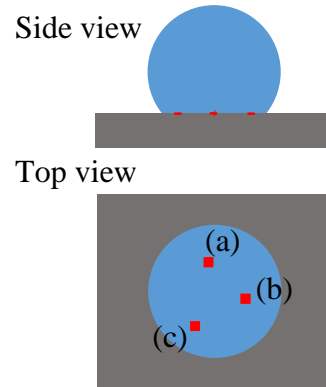


Fig. s3 Schematic diagram of solid fraction measurement areas at porous Si surface.

For example, a histogram of pore diameter distribution can be obtained based on the surface image as shown in Fig. s2. Therefore, the total pore area A_{pore} in the given area A of the surface image can be obtained by integrating the area of each pore.

Since the surface image area is limited for image analysis, the solid fraction has been measured several times in the area where the droplet is placed, in order to confirm if the solid fraction is uniform at the surface. As shown in Fig. s3, the local solid fraction of different areas (in red) on the surface can be used to calculate the mean solid fraction.

Examples of the local surface images and pore diameter histograms at three different areas on the porous Si surface are shown in Fig. s4. The image area is $7490 \mu\text{m}^2$, and the local solid fractions are obtained to be 0.703, 0.701 and 0.686, resulting in a mean solid fraction of $\Phi=0.697$. The standard deviation in this case is 9.29×10^{-3} .

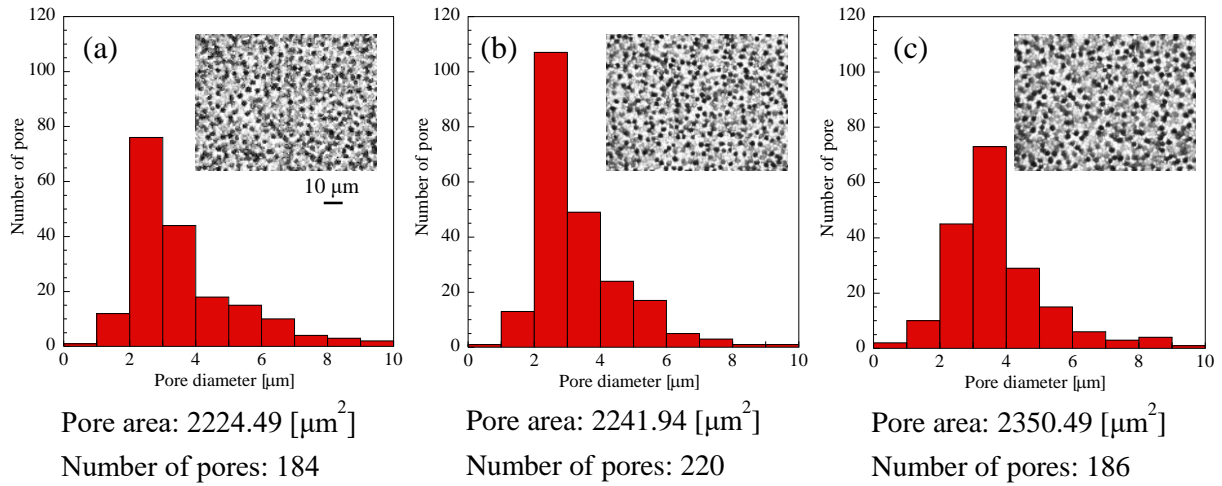


Fig. s4 Comparisons of surface images and pore diameter distributions at different measurement areas at porous Si surface of mean solid fraction $\Phi= 0.697$.

3. Fractal dimension D

The fractal dimension analysis is based on the traditional box counting method for the 2D surface images. The reason of using the box counting method is that using the different method will lead to difficulties in comparing the results (because each method gives slightly different results when analyzing the same structure) and the box counting method is the most commonly used method for fractal dimension analysis of real objects in practice (For example, F. K. et al., *Appl. Math. Comput.* 1999, 105, 195-210; L. J. et al., *Pattern Recognit.* 2009, 42, 2460-2469; S. N. and C. B. B., *IEEE Trans. Cybern.* 1994, 24, 115-120.). With the aid of fractal analysis software [<http://cse.naro.affrc.go.jp/sasaki/fractal/fractal.html>, fractal3, Ver. 3.4.7], the fractal dimension D is obtained from the gray scale images by box counting method defined as

$$D = \frac{\log_{10} N}{\log_{10} \delta} \quad (b)$$

where N is the number of boxes that cover the surface, and δ is the magnification (i.e. the inverse of the box size). Figs. s5 and s6 show the typical analyzed surface images and the results of Eq. (b) to calculate the fractal dimensions at the porous and patterned Si surfaces. The details of the individual fractal dimension for the 9 samples shown in Figures 3 and 5 are summarized in the Table s1. For the porous Si surfaces shown in Figure 3, the mean fractal dimension is approximate to 2.40 and the standard deviation is 0.023. For the patterned Si surfaces having the similar structures with different parameters of a or s shown in Figure 5, the mean fractal dimension is 2.19 and the standard deviation of the fractal dimension is 0.028.

Table s1. Fractal dimension D of sample surfaces shown in Figures 3 & 5.

Samples	a	b	c	d	e
D of Porous Si (Figure 3)	2.4238	2.4183	2.4070	2.3986	2.3645
D of Patterned Si (Figure 5)	2.2195	2.1673	2.1609	2.2008	

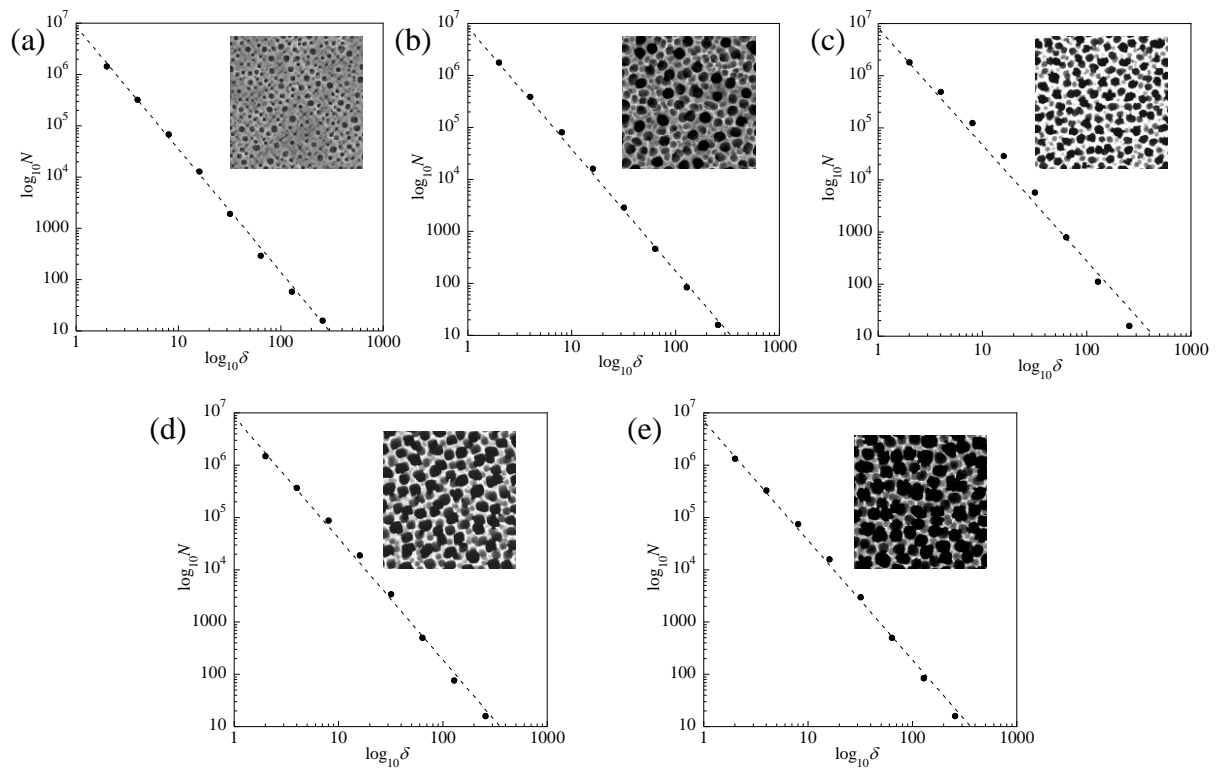


Fig. s5 Fractal dimension analysis examples based on box counting method for porous Si surface.

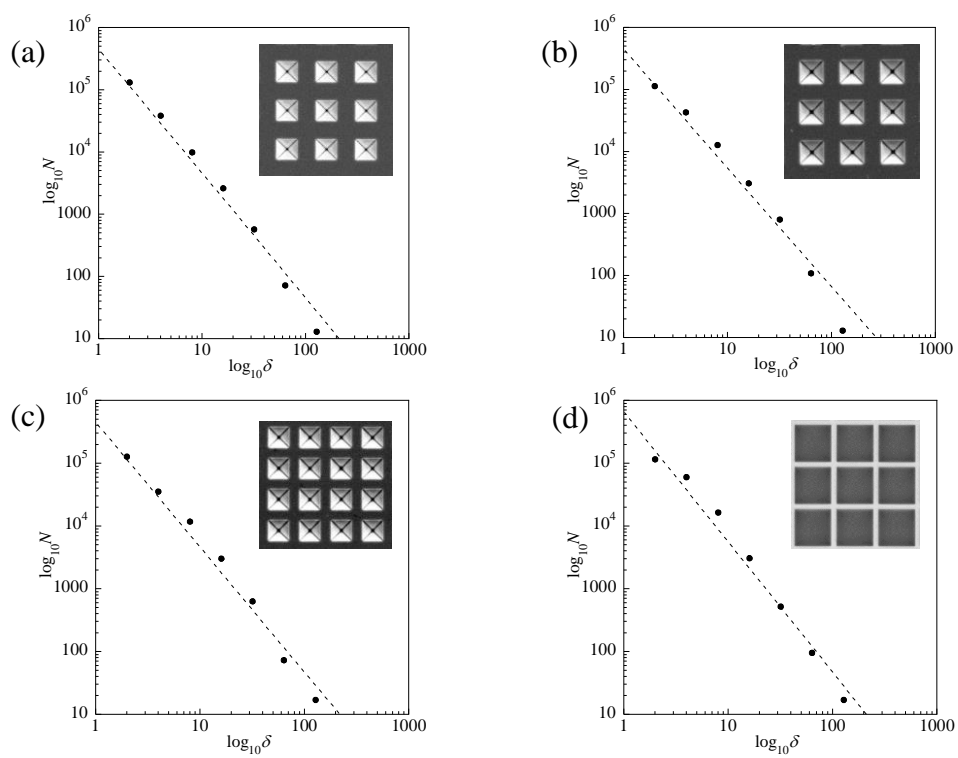


Fig. s6 Fractal dimension analysis examples based on box counting method for patterned Si surface.

4. Experimental method on the measurement of contact angle at structured Si surface

The contact angle is measured using $\theta/2$ method. Geometrically, the liquid drop is assumed to be part of a sphere as shown in Fig. s7. Thus, the contact angle can be calculated by measuring the drop diameter and the height.



Fig. s7 Schematic of contact angle measurement by $\theta/2$ method

The measurement of contact angles at structured Si surfaces was prepared carefully to avoid both the oxide layer and the contamination on the surfaces. The Si samples, illustrated in the schematic diagram in Fig. s8, have the etched area (with different surface structures) and the un-etched area (flat surface). Every sample has been immersed into the acetone solutions to remove dirt (including the contaminations), and the buffered hydrofluoric acid solutions to remove silicon oxide film, and rinsed by the pure water repeatedly. The contact angle at the un-etched area for every sample has been confirmed to be the same to the θ_Y ($79.5^\circ \pm 0.5^\circ$), which means that all of the samples have the same chemical compositions. Furthermore, the measurement of contact angle has been carried out within 10 minutes after surface cleaning, covered with a measurement cell.

Sample preparation procedures

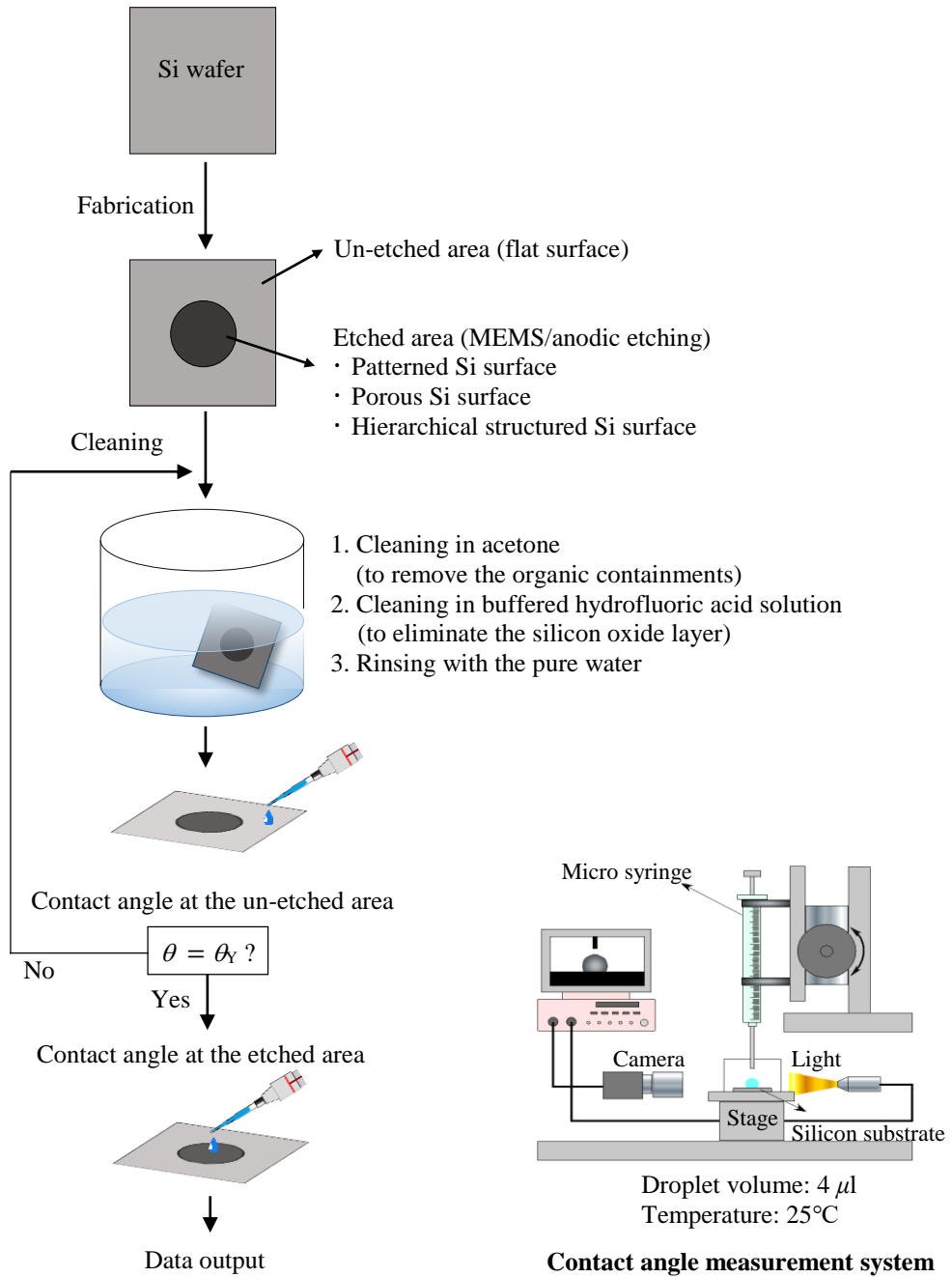


Fig. s8 Schematic diagram of sample preparation and contact angle measurement system.

5. Static intermediate wetting state

The typical time history of static contact angle is shown in Fig. s9 in comparison to that of reducing contact angle during droplet evaporation. It is clear that the static contact angles keep in constant, i.e. the intermediate wetting state measured under the equilibrium condition exists stable. No significant evidence could be found on the spontaneous wetting transition between the Wenzel and Cassie-Baxter states.

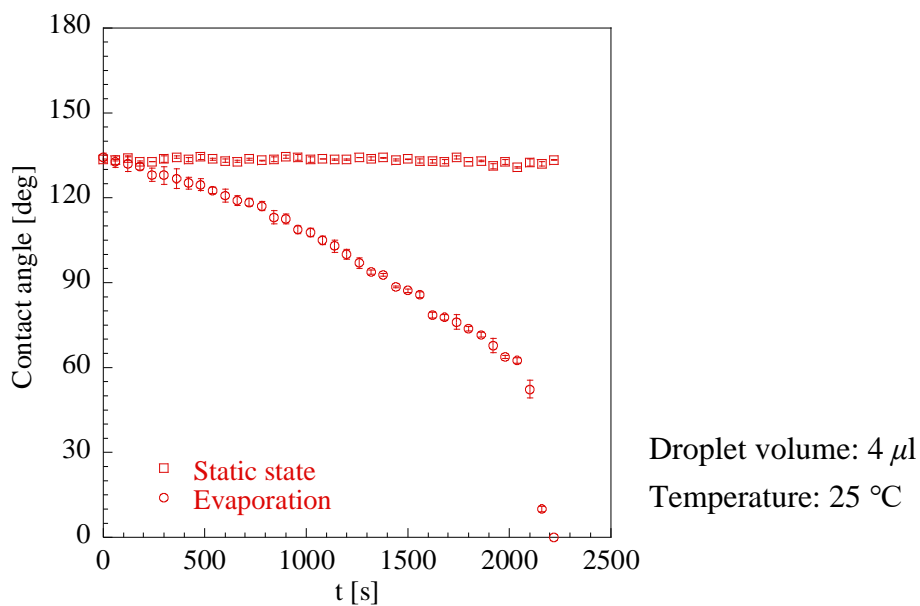


Fig. s9 Typical time history of measured water contact angles in equilibrium condition (open squares) and in evaporation (open circles).